First-order phase transitions in scalar electrodynamics

W. Buchmüller, T. Helbig and D. Walliser

Deutsches Elektronen-Synchrotron DESY, W-2000 Hamburg 52, Germany

We investigate in detail the transition from the symmetric to the broken phase in scalar electrodynamics at finite temperature. Our analysis is based on the effective potential to order e^3 and $\lambda^{3/2}$, where e and λ are the gauge coupling and scalar self-coupling, respectively. Plasma masses of scalar and vector fields are determined from a set of one-loop gap equations which also yield the range in e, λ and temperature T, where perturbation theory is consistent. We determine the values of e and λ for which the symmetric phase is metastable. Depending on the convergence of the perturbation series, for a vector boson mass of 90 GeV the Higgs boson mass may be as large as 120 GeV. Following the theory of Langer we calculate the nucleation rate of critical droplets and determine the temperature at which a cosmological phase transition would be completed. For large vector boson and Higgs boson masses the phase transition is weakly first order.

1. Introduction

The standard model of particle physics describes strong and electroweak interactions correctly down to distances of order 10^{-16} cm or equivalently, up to energies of order 100 GeV. An important postdiction of the standard model is the occurrence of a phase transition in the very early universe at a critical temperature of order 100 GeV, above which the gauge symmetry of weak and electromagnetic interactions is restored [1–4]. This electroweak phase transition has recently attracted much attention. It is of crucial importance for the baryon asymmetry of the universe, since baryon- and lepton-number violating processes fall out of thermal equilibrium at the corresponding critical temperature [5]. If the cosmological phase transition was first order, relics may have been left over due to departure from thermal equilibrium. In particular, it is then conceivable that the baryon asymmetry of the universe was produced primordially at the electroweak scale.

Several important steps towards a theory of the electroweak phase transition have already been made [6–8], although a fully satisfactory quantitative description of the phase transition is still lacking. To a large extent this is due to problems caused by infrared divergencies which plague perturbation theory in finite-temperature field theory. These infrared problems are manifest, for instance, in spurious

terms linear in the scalar field ϕ [9,10], which appear in separate contributions to the effective potential, but cancel in the complete expression. Other open questions concern the decay of metastable states, i.e., nucleation, growth and coalescence of critical droplets. Furthermore, in the case of a weak first-order transition one has to worry about the importance of subcritical droplets and large thermal fluctuations [11–14].

In this paper we shall address some of these problems in the context of scalar electrodynamics at finite temperature where the interesting possibility of a first-order phase transition was considered already many years ago [15,16]. This theory is much simpler than the standard model of electroweak interactions but it already exhibits most of the problems related to infrared divergencies. The paper is organized as follows. In sect. 2 we calculate the effective potential to order e^3 and demonstrate explicitly the cancellation of spurious linear terms. We also discuss the breakdown of ordinary perturbation theory and the necessity of an improved perturbation theory where plasma masses are incorporated from the beginning. Sect. 3 deals with the vector boson propagator at finite temperature, in particular with the relation between longitudinal and transverse plasma masses and the self-energy tensor in the case of spontaneous symmetry breaking. In sect. 4 we then obtain the complete set of one-loop gap equations. We evaluate the effective potential to order e^3 and $\lambda^{3/2}$, and estimate the range in e, λ and temperature T, where the potential is reliable. This allows us to determine a region in the plane of couplings (e^2, λ) for which the symmetric phase is metastable. Following the theory of Langer [17,18] we compute the nucleation rate of critical droplets in sect. 5. We also determine the temperature at which a cosmological phase transition would be completed and discuss the strength of the first-order transition. Our results are summarized in sect. 6.

2. Breakdown of perturbation theory

Perturbation theory of scalar electrodynamics at finite temperature is based on the action *

$$S_\beta[\Phi, A] = \int_\beta \mathrm{d}x \left(-\tfrac{1}{4} F_{\mu\nu} F^{\mu\nu} + |D_\mu \Phi|^2 - V_0(\sqrt{2\Phi^*\Phi}) \right), \tag{1}$$

where

$$\int_\beta \mathrm{d}x \equiv \int_0^\beta \mathrm{d}\tau \int \mathrm{d}^3 x, \quad \beta = \frac{1}{T}, \quad D_\mu = \partial_\mu - ieA_\mu, \tag{2}$$

$$V_0 = \mu \Phi^* \Phi + \lambda (\Phi^* \Phi)^2, \quad \mu < 0. \tag{3}$$
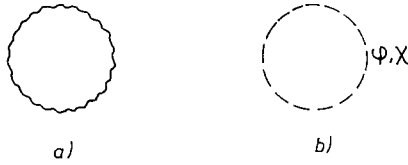
---

* We use the conventions of ref. [19].

Fig. 1. One-loop contributions to the effective potential.

The complex scalar field $\Phi = (1/\sqrt{2})(\phi + i\chi)$ contains Higgs and Goldstone boson fields ϕ and χ respectively, $F_{\mu\nu}$ is the field strength of the vector field A_μ and e is the gauge coupling. $v = \sqrt{-\mu/\lambda} = v^*$ is the zero-temperature vacuum expectation value of $\sqrt{2}\,\Phi$. The free energy $F[\Phi, T]$ can now be expressed in terms of a functional integral over the shifted action S_β (cf. ref. [20]):

$$e^{-\beta F[\Phi, T]} = \int_\beta [D\hat{\Phi}][DA_\mu]\,\delta(f)\,\det\frac{\partial f}{\partial \alpha}$$

$$\times \exp\left(-S_\beta\big[\Phi + \hat{\Phi}, A_\mu\big] - \int_\beta dx \frac{\delta F[\Phi, T]}{\delta \Phi(x)}\hat{\Phi}(x)\right), \qquad (4)$$

where f is a gauge fixing condition for the gauge field. In this paper we choose the Landau gauge. The functional integration is over periodic fields, i.e., $\Phi(0, x) = \Phi(\beta, x)$ and $A_\mu(0, x) = A_\mu(\beta, x)$.

For constant background fields $F[\Phi, T]$ is identical with the finite-temperature effective potential and in the one-loop approximation one finds (cf. fig. 1, refs. [15,19])

$$F\left[\frac{\phi}{\sqrt{2}}, T\right] \equiv V(\phi, T) = V_0(\phi) + V_1(\phi, T)$$

$$= -\tfrac{2}{45}\pi^2 T^4 - \tfrac{1}{12}\lambda v^2 T^2 + \tfrac{1}{2}\big[\tfrac{1}{12}(3e^2 + 4\lambda)T^2 - \lambda v^2\big]\phi^2$$

$$- \frac{1}{12\pi}\Big[3e^3\phi^3 + \lambda^{3/2}(3\phi^2 - v^2)^{3/2} + \lambda^{3/2}(\phi^2 - v^2)^{3/2}\Big]T + \tfrac{1}{4}\lambda\phi^4$$

$$+ \frac{1}{64\pi^2}\Big[3e^4\phi^4 + \lambda^2(3\phi^2 - v^2)^2 + \lambda^2(\phi^2 - v^2)^2\Big]\ln\frac{T^2}{M^2}. \qquad (5)$$

Here, in the high-temperature expansion, terms up to order $(m_i/T)^3$ have been kept, where the tree-level vector boson mass m, the Higgs mass $\overline{m}_\phi$ and the Goldstone boson mass $\overline{m}_\chi$ are given by

$$m^2 = e^2\phi^2, \quad \overline{m}_\phi^2 = \lambda(3\phi^2 - v^2), \quad \overline{m}_\chi^2 = \lambda(\phi^2 - v^2). \qquad (6)$$

Note that $\overline{m}_\phi^2$ and $\overline{m}_\chi^2$ are negative for small values of ϕ.

Let us first ignore the terms of order $\lambda^{3/2}$ in eq. (5) which may be justified for $\lambda \ll e^2$ and recall the qualitative features of the free energy. As a result of the finite-temperature corrections the second derivative of the effective potential at the origin becomes positive for temperatures above the "barrier temperature" T_b,

$$T_b^2 = \frac{12\lambda v^2}{3e^2 + 4\lambda}. \tag{7}$$

Hence, for $T > T_b$ the symmetric phase is a local minimum of the effective potential. From eq. (5) one easily finds that for temperatures close enough to T_b, which satisfy the upper bound

$$\frac{T^2 - T_b^2}{T^2} \leqslant \frac{27e^6}{16\pi^2\lambda(3e^2 + 4\lambda)}, \tag{8}$$

two other extrema exist:

$$\phi_\pm(T) = \frac{3e^3}{8\pi\lambda} T \left(1 \pm \sqrt{1 - \frac{16\pi^2\lambda(3e^2 + 4\lambda)}{27e^6} \frac{T^2 - T_b^2}{T^2}}\right). \tag{9}$$

ϕ_- corresponds to a local maximum of F and ϕ_+ is a second local minimum which at the critical temperature T_c, where

$$\frac{T_c^2 - T_b^2}{T_c^2} = \frac{3e^6}{2\pi^2\lambda(3e^2 + 4\lambda)}, \tag{10}$$

is degenerate with $\phi = 0$. The global minimum of the free energy is ϕ_+ for temperatures below T_c whereas it is the symmetric phase $\phi = 0$ for temperatures above T_c. Note, that the second minimum ϕ_+ occurs due to a compensation between terms of order λ and e^3.

Our determination of the critical temperature is based on the effective potential in the high-temperature expansion, which breaks down for $m(\phi_c) = e\phi_c > T_c$, where $\phi_c = \phi_+(T_c)$. Together with eqs. (9) and (10) this implies for λ the lower bound

$$\lambda > \frac{e^4}{2\pi}. \tag{11}$$

Note that this condition is much more stringent than the Weinberg–Linde bound $\lambda > 3e^4/(32\pi^2)$ [21]. The lower bound on λ provides upper bounds for the critical temperature T_c and the critical field ϕ_c:

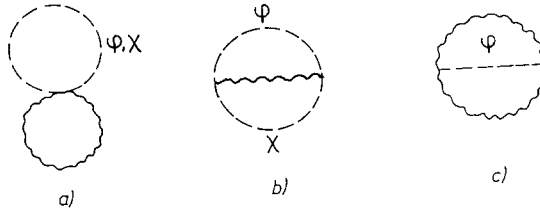$$\frac{T_c^2 - T_b^2}{T_c^2} < \frac{1}{\pi}, \quad \frac{\phi_c^2}{v^2} < \frac{2}{\pi - 1}. \tag{12}$$

Fig. 2. Two-loop contributions to the effective potential. (Vector loops only.)

As expected, the expectation value ϕ_c at T_c is smaller than the vacuum expectation value v at $T = 0$. Due to the barrier in the effective potential, generated by quantum fluctuations, the symmetry breaking phase transition appears to be first order with a strength which depends on the ratio λ/e^2 of coupling constants.

To what extend can we trust this result? For our calculation we needed the effective potential for values of ϕ between 0 and ϕ_c. But finite-temperature perturbation theory is well known to yield in higher orders terms proportional to $(eT/m(\phi))^n = (T/\phi)^n$, i.e., the series is badly divergent for small values of ϕ. A manifestation of these infrared divergencies is the appearance of terms linear in ϕ in the effective potential. The two-loop graphs shown in figs. 2a, b yield the linear terms

$$V_2^{(a)}(\phi, T) = -\frac{e^3}{16\pi}T^3\phi + \ldots, \tag{13}$$

$$V_2^{(b)}(\phi, T) = \frac{e^3}{48\pi}T^3\phi + \ldots. \tag{14}$$

Clearly, a linear term in the effective potential would invalidate our previous discussion.

The most infrared divergent contributions in higher orders arise from ring diagrams (cf. fig. 3, refs. [8,19,22]). Their sum yields the contribution to the effective potential

$$V_1 + V_{\text{RING}}$$

$$= -\tfrac{1}{2}\int_\beta \mathrm{d}p \left(\ln\left(p^2 - m_{\text{L}}^2 \right) + 2\ln\left(p^2 - m_{\text{T}}^2 \right) \right.$$

$$\left. - \frac{\delta m_{\text{L}}^2}{p^2 - m^2} - 2\frac{\delta m_{\text{T}}^2}{p^2 - m^2} \right), \tag{15}$$

where m_{L} (m_{T}) is the longitudinal (transverse) plasma mass of the photon propagator and δm_{L}^2 (δm_{T}^2) is the deviation from the tree-level mass, i.e., $m_{\text{L,T}}^2 =$
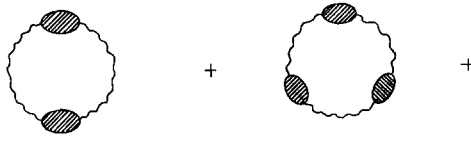
Fig. 3. Ring diagram contributions to the effective potential. (Vector loops only.)

$m^2 + \delta m_{L,T}^2$. Here we have anticipated the structure of the photon propagator which will be discussed in detail in the following section. For the one-loop plasma masses we find (cf. fig. 4)

$$\delta m_L^2 = \frac{e^2}{3} T^2 - \frac{e^3}{\pi} T\phi + \ldots, \tag{16}$$

$$\delta m_T^2 = \qquad - \frac{2e^3}{3\pi} T\phi + \ldots. \tag{17}$$

The integral (15) is easily evaluated. One obtains

$$V_1 + V_{\text{RING}} = -\tfrac{2}{45}\pi^2 T^4 + \tfrac{1}{8}e^2 T^2 \phi^2$$

$$- \frac{1}{12\pi} \left[m_L^3 + 2m_T^3 - \tfrac{3}{2}m\left(\delta m_L^2 + 2\delta m_T^2\right) \right] T$$

$$+ \frac{1}{64\pi^2} \left[m_L^4 + 2m_T^4 - 2m^2\left(\delta m_L^2 + \delta m_T^2\right) \right] \ln \frac{T^2}{M^2}. \tag{18}$$

The result contains a term linear in ϕ which, to leading order in e, is given by

$$\frac{3e}{24\pi}\delta m_L^2 \phi T = \frac{e^3}{24\pi} T^3 \phi + \ldots. \tag{19}$$

Hence, the ring diagram contribution precisely cancels the sum of the two-loop terms $V_2^{(a)} + V_2^{(b)}$ (cf. eqs. (13) and (14)) to leading order in e. One expects that the linear terms of higher order in e are also spurious and cancel if all contributions to
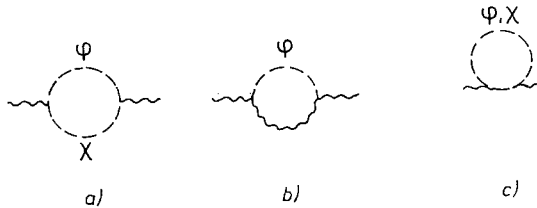

Fig. 4. One one-loop contributions to the photon plasma masses.

the effective potential are summed, but, to our knowledge, this hope has not been proven so far.

Summing the "daisy" graphs [3], i.e., the ring diagrams with one-loop self-energy insertions, had lead to a cancellation of linear terms. However, a new problem has appeared. According to eq. (17), at small values of ϕ,

$$\phi < \frac{2e}{3\pi} T, \tag{20}$$

the transverse plasma mass square m_T^2 becomes negative and perturbation theory appears to break down! As we shall see in the following sections, this problem is cured if the plasma masses of the scalar fields are also taken into account. This is needed anyhow since to order $\lambda^{3/2}$ the one-loop approximation breaks down for all values of ϕ between zero and $\phi_c < v$! A self-consistent determination of all plasma masses by means of gap equations amounts to summing "daisy" and "superdaisy" graphs for the effective potential and will be carried out in sect. 4.

3. Improved perturbation theory

In order to determine the plasma masses of vector and scalar fields, we first have to discuss the structure of the vector propagator at finite temperature. The photon self-energy $\Pi_{\mu\nu}(k)$ depends on the photon four-momentum k^μ and the four-vector $u^\mu = (1, \mathbf{0})$ which specifies the rest frame of the system (cf. ref. [19]). Hence, in general $\Pi_{\mu\nu}$ is a linear combination of four tensors. A convenient choice is

$$P_{T\mu\nu} = g_\mu{}^i \left(\delta_{ij} - \frac{k_i k_j}{k^2} \right) g^j{}_\nu, \tag{21}$$

$$P_{L\mu\nu} = \frac{k_\mu k_\nu}{k^2} - g_{\mu\nu} - P_{T\mu\nu} = \frac{k^2}{k^2} u_\mu^T u_\nu^T, \tag{22}$$

$$P_{G\mu\nu} = -\frac{k_\mu k_\nu}{k^2}, \tag{23}$$

$$S_{\mu\nu} = \frac{1}{\sqrt{2k^2}} \left(k_\mu u_\nu^T + k_\nu u_\mu^T \right), \tag{24}$$

where $u_\mu^T = u_\mu - k_\mu (u \cdot k)/k^2$ is transverse, $u_\mu^T k^\mu = 0$. These tensors satisfy the relations

$$P_T^2 = -P_T, \quad P_L^2 = -P_L, \quad P_G^2 = -P_G, \quad S^2 = \tfrac{1}{2}(P_L + P_G), \tag{25}$$

$$P_T P_L = P_T P_G = P_L P_G = SP_T = P_L SP_L = 0, \tag{26}$$

$$P_{T\mu}{}^\mu = 2P_{L\mu}{}^\mu = 2P_{G\mu}{}^\mu = -2, \quad S_\mu{}^\mu = 0. \tag{27}$$

In Landau gauge, where the bare propagator is transverse,

$$D(k) = \frac{-1}{k^2 - m^2}(P_L + P_T),\tag{28}$$

the photon self-energy tensor

$$\Pi(k) = \Pi_L(k)P_L + \Pi_T(k)P_T + \Pi_S(k)S + \Pi_G(k)P_G\tag{29}$$

yields the full propagator

$$\tilde{D}(k) = \sum_{n=0}^{\infty} D(k)(\Pi(k)D(k))^n$$

$$= \frac{-1}{k^2 - m^2 - \Pi_L(k)}P_L + \frac{-1}{k^2 - m^2 - \Pi_T(k)}P_T.\tag{30}$$

Due to the relations (25) and (26) the full propagator does not depend on $\Pi_S(k)$ and $\Pi_G(k)$.

However, knowledge of Π_G is important since it enters in the relations which yield the longitudinal and transverse plasma masses:

$$\delta m_L^2 = \Pi_L(0) = \text{Tr}(\Pi(0)P_L) = -\Pi_{00}(0),\tag{31}$$

$$\delta m_T^2 = \Pi_T(0) = \tfrac{1}{2}\text{Tr}(\Pi(0)P_T) = -\tfrac{1}{2}(\Pi^\mu{}_\mu(0) + \Pi_L(0) + \Pi_G(0)),\tag{32}$$

where

$$\Pi_G(k) = \text{Tr}(\Pi(k)P_G).\tag{33}$$

Here $\Pi_{\mu\nu}(0)$ is defined by setting first $k_0 = 0$ and then performing the limit $k^2 \to 0$. In gauge theories with unbroken symmetry one has $\Pi_G = 0$ in Landau gauge. Note, that this is *not* the case if the symmetry is spontaneously broken. As eq. (32) shows this fact is important in order to extract the correct transverse mass from $\Pi_{\mu\nu}$.

In scalar electrodynamics the one-loop photon self-energy corrections are given by figs. 7a–c. The corresponding integral reads

$$\Pi_{\mu\nu}(k) = e^2 \int_\beta dq \left\{ \frac{1}{q^2 - m_\phi^2} \left[\frac{1}{(q+k)^2 - m_\chi^2}(2q+k)_\mu(2q+k)_\nu \right.\right.$$

$$\left.\left. - \frac{4m^2}{(q+k)^2 - m^2}\left(g_{\mu\nu} - \frac{(q+k)_\mu(q+k)_\nu}{(q+k)^2}\right)\right] \right.$$

$$\left. - g_{\mu\nu}\left(\frac{1}{q^2 - m_\phi^2} + \frac{1}{q^2 - m_\chi^2}\right) \right\}.\tag{34}$$

Using eqs. (29)–(33) we find, including terms up to $\ln(m_i^2/T^2)$,

$$\delta m_{\rm L}^2 = \tfrac{1}{3}e^2 T^2 - \frac{e^2}{4\pi}\left(4\frac{m^2}{m+m_\phi}+m_\phi+m_\chi\right)T$$

$$-\frac{3e^2}{16\pi^2}\frac{m^2}{m^2-m_\phi^2}\left(m^2\ln\frac{m^2}{T^2}-m_\phi^2\ln\frac{m_\phi^2}{T^2}\right), \qquad (35)$$

$$\delta m_{\rm T}^2 = -\frac{e^2}{12\pi}\left(8\frac{m^2}{m+m_\phi}-\frac{(m_\phi-m_\chi)^2}{m_\phi+m_\chi}\right)T$$

$$-\frac{3e^2}{16\pi^2}\frac{m^2}{m^2-m_\phi^2}\left(m^2\ln\frac{m^2}{T^2}-m_\phi^2\ln\frac{m_\phi^2}{T^2}\right). \qquad (36)$$

With $m_\phi=m_\chi=0$ and ignoring terms $O(\ln(m_i/T))$ one obtains eqs. (16) and (17).

For small values of ϕ the temperature-dependent plasma mass corrections $\delta m_{\rm L,T}^2$ can become larger than the tree-level mass m^2. This suggests an improved perturbation theory, where loop diagrams are evaluated with propagators containing the exact masses $m_{\rm L,T}^2 = m^2 + \delta m_{\rm L,T}^2$, $m_{\phi,\chi}^2 = \overline{m}_{\phi,\chi}^2 + \delta m_{\phi,\chi}^2$. The radiative corrections are treated as counter terms,

$$\delta S_\beta = -\tfrac{1}{2}\int_\beta \mathrm{d}p\left[\tilde{A}^\mu(p)\left(\delta m_{\rm L}^2 P_{{\rm L}\mu\nu}+\delta m_{\rm T}^2 P_{{\rm T}\mu\nu}\right)\tilde{A}^\nu(p)\right.$$

$$\left.-\delta m_\phi^2\tilde{\phi}^2(p)-\delta m_\chi^2\tilde{\chi}^2(p)\right], \qquad (37)$$

and are determined self-consistently by solving gap equations at the corresponding loop order. To order e^3, $\delta m_{\rm L}^2$ and $\delta m_{\rm T}^2$ are given by eqs. (35) and (36).

It is instructive to study in this framework the cancellation of linear terms which appear in separate contributions to the effective potential. The one-loop graphs shown in figs. 5a, b yield

$$V_1 = -\tfrac{2}{45}\pi^2 T^4 + \tfrac{1}{8}e^2 T^2\phi^2$$

$$-\frac{1}{12\pi}\left(m_{\rm L}^3+2m_{\rm T}^3-\tfrac{3}{2}m_{\rm L}\delta m_{\rm L}^2-3m_{\rm T}\delta m_{\rm T}^2\right)T$$

$$+\frac{1}{64\pi^2}\left(m_{\rm L}^4+2m_{\rm T}^4-2m_{\rm L}^2\delta m_{\rm L}^2-4m_{\rm T}^2\delta m_{\rm T}^2\right)\ln\frac{T^2}{M^2}. \qquad (38)$$

This result is very similar to eq. (18), the sum of one-loop and ring diagrams $V_1+V_{\rm RING}$ in ordinary perturbation theory. Note, however, that the term $m\delta m_{\rm L}^2$

Fig. 5. One-loop contribution to the effective potential with full photon propagators including counterterms. (Vector loops only.)

in eq. (18) which gave the linear term to order e^3, has been replaced by

$$m_L \delta m_L^2 = \frac{e^3}{3\sqrt{3}} T^3 \left(1 + \frac{3}{2} \frac{\phi^2}{T^2} + O(e) \right). \tag{39}$$

Hence, V_1 does not yield a linear term to order e^3. For the two two-loops shown in figs. 6a, b we find

$$V_2^{(a)} = -\frac{e^3}{24\pi} T^3 \phi + \dots = -V_2^{(b)} + \dots. \tag{40}$$

Hence, to leading order in e the two-loop contributions compensate each other and there is no need to sum up an infinite series of ring diagrams to achieve the cancellation. This is expected since the leading infrared divergencies are eliminated by the longitudinal plasma mass of the vector boson and the subtractions due to the counter terms δm_L^2 and δm_T^2. In order to discuss subleading infrared divergencies the gap equations have to be studied at finite momentum.

It is straightforward to show that an equivalent cancellation occurs for all scalar loops to $O(\lambda^{3/2})$. Therefore the effective potential

$$V(\phi, T) = cT^4 + \tfrac{1}{2}\left(\tfrac{1}{4} e^2 + \tfrac{1}{3}\lambda \right)\left(T^2 - T_b^2 \right)\phi^2 + \tfrac{1}{4}\lambda\phi^4$$

$$- \left(m_L^3 + 2m_T^3 + m_\phi^3 + m_\chi^3 \right)\frac{T}{12\pi} + O(e^4, \lambda^2) \tag{41}$$

does not have a term linear in ϕ to $O(e^3)$ and $O(\lambda^{3/2})$.
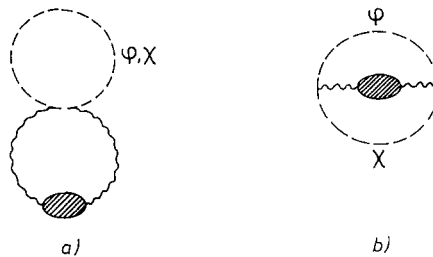

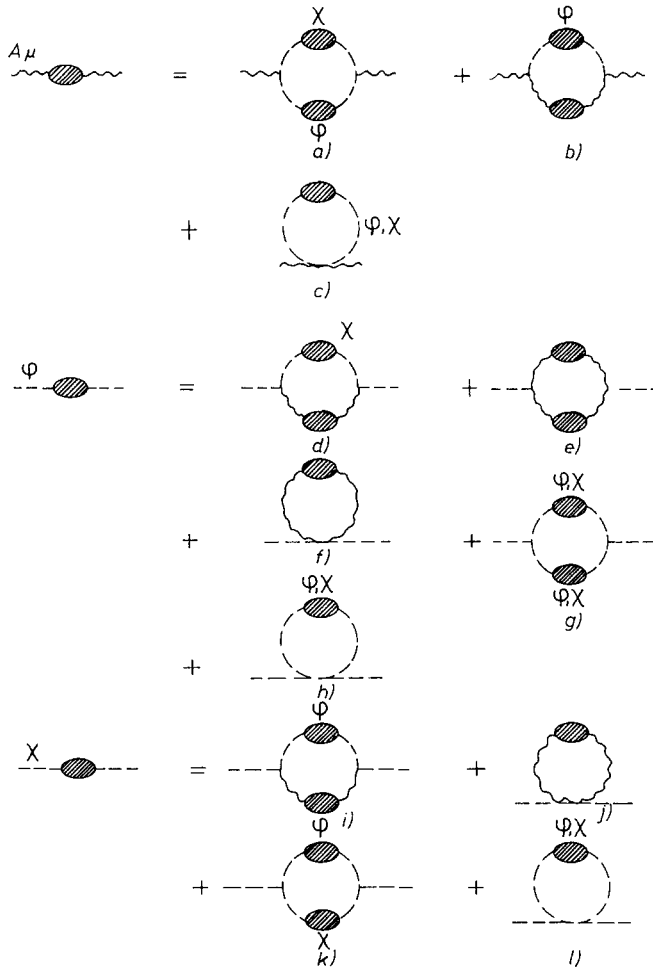Fig. 6. Two-loop contributions to the effective potential with full photon propagators. (Vector loops only.)

Fig. 7. The gap equations: All one-loop self-energy corrections with full propagators.

4. The gap equations

Let us now investigate the phase structure of scalar electrodynamics by means of the one-loop gap equations. The corresponding graphs are shown in fig. 7. A straightforward calculation yields the following set of equations:

$$m_L^2 = \tfrac{1}{3}e^2T^2 + m^2 - \frac{e^2}{4\pi}\left(\frac{4m^2}{m_L + m_\phi} + m_\phi + m_\chi\right)T, \qquad (42)$$

$$m_T^2 = m^2 - \frac{e^2}{12\pi}\left(\frac{8m^2}{m_T + m_\phi} - \frac{(m_\phi - m_\chi)^2}{m_\phi + m_\chi}\right)T, \qquad (43)$$

$$m_\phi^2 = \left(\tfrac{1}{4}e^2 + \tfrac{1}{3}\lambda\right)\left(T^2 - T_b^2\right) + 3\overline{m}^2 - \frac{e^2}{4\pi}\left[m_L + 2m_T + m^2\left(\frac{1}{m_L} + \frac{2}{m_T}\right)\right]T$$

$$- \frac{\lambda}{4\pi}\left[3m_\phi + m_\chi + \overline{m}^2\left(\frac{9}{m_\phi} + \frac{1}{m_\chi}\right)\right]T, \tag{44}$$

$$m_\chi^2 = \left(\tfrac{1}{4}e^2 + \tfrac{1}{3}\lambda\right)\left(T^2 - T_b^2\right) + \overline{m}^2$$

$$- \frac{e^2}{4\pi}(m_L + 2m_T)T - \frac{\lambda}{4\pi}\left(m_\phi + 3m_\chi + \frac{4\overline{m}^2}{m_\phi + m_\chi}\right)T, \tag{45}$$

where

$$m = e\phi, \quad \overline{m} = \sqrt{\lambda}\,\phi, \quad T_b^2 = \frac{12\lambda v^2}{3e^2 + 4\lambda}. \tag{46}$$

Here we have neglected terms of order $\ln(m_i/T)$ in the high-temperature expansion.

It is instructive to consider the gap equations for the pure scalar theory ($e = 0$) and at $\phi = 0$. From eqs. (44) and (45) one obtains for temperatures close to the barrier temperature:

$$m_\phi \sim m_\chi \sim \tfrac{2}{3}\pi(T - T_b), \tag{47}$$

i.e., m_ϕ and m_χ approach zero with critical index one. This well-known result was first obtained by Dolan and Jackiw in the large-N limit [3]. We obtain the same result since at $\phi = 0$ only graphs (h) and (l) of fig. 7 contribute, which are the leading terms in a $(1/N)$-expansion. The behaviour of m_ϕ and m_χ for small values of ϕ at $T = T_b$ cannot be obtained from eqs. (44) and (45) as m_ϕ and m_χ are only $O(1/N)$ in this case, and graphs (g) and (k) of fig. 7 contribute to the same order. Due to these graphs perturbation theory breaks down for temperatures T close to T_b. Consequently, eq. (47) cannot be expected to hold in our case where $N = 2$.

From the gap equations (42)–(45) one can determine the plasma masses to $O(e^3, \lambda^{3/2})$. They are easily found by inserting the lowest order results

$$m_L^0 = \sqrt{\tfrac{1}{3}e^2 T^2 + m^2},$$

$$m_T^0 = m,$$

$$m_\phi^0 = \sqrt{\left(\tfrac{1}{4}e^2 + \tfrac{1}{3}\lambda\right)\left(T^2 - T_b^2\right) + 3\overline{m}^2},$$

$$m_\chi^0 = \sqrt{\left(\tfrac{1}{4}e^2 + \tfrac{1}{3}\lambda\right)\left(T^2 - T_b^2\right) + \overline{m}^2}, \tag{48}$$

into the RHS of the gap equations. From the scalar masses m_ϕ^2 and m_χ^2 one can derive the effective potential by integration. Note, that due to the global U(1)-symmetry of our theory the potential is only a function of $\sqrt{2\Phi^*\Phi} = \sqrt{\phi^2 + \chi^2}$. Hence, at $\chi = 0$, the masses $m_\phi(\phi, T)$ and $m_\chi(\phi, T)$ are given by

$$m_\phi^2(\phi, T) = \frac{\partial^2 V(\phi, T)}{\partial \phi^2},\tag{49}$$

$$m_\chi^2(\phi, T) = \frac{1}{\phi}\frac{\partial V(\phi, T)}{\partial \phi},\tag{50}$$

and thus

$$V(\phi, T) = \int^\phi d\phi' \, \phi' m_\chi^2(\phi', T_b)$$

$$= cT^4 + \tfrac{1}{2}\left(\tfrac{1}{4}e^2 + \tfrac{1}{3}\lambda\right)\left(T^2 - T_b^2\right)\phi^2 + \tfrac{1}{4}\lambda\phi^4$$

$$- \left(m_L^{0^3} + 2m_T^{0^3} + m_\phi^{0^3} + m_\chi^{0^3}\right)\frac{T}{12\pi} + O(e^4, \lambda^2).\tag{51}$$

As expected, there are no terms linear in ϕ and eq. (51) coincides with eq. (41) to the order in which we are working. The evaluation of the effective potential to $O(e^4, \lambda^2)$ requires to incorporate two-loop contributions in eqs. (42)–(45), and in order to obtain the exact effective potential the gap equations have to be replaced by the full Schwinger–Dyson equations.

Under which conditions is the perturbative expansion valid? At the origin, $\phi = 0$, the curvature of the potential $m_\phi^2(\phi, T)$ is positive if

$$m_\phi^2 = \left(\tfrac{1}{4}e^2 + \tfrac{1}{3}\lambda\right)\left(T^2 - T_b^2\right) - \frac{e^3}{4\sqrt{3}\,\pi}T^2 - \frac{\lambda T}{\pi}\sqrt{\left(\tfrac{1}{4}e^2 + \tfrac{1}{3}\lambda\right)\left(T^2 - T_b^2\right)} \geqslant 0.\tag{52}$$

This implies the corrected barrier temperature

$$T_b'^2 = \frac{12\lambda v^2}{3e^2 + 4\lambda - \sqrt{3}\,e^3/\pi}\left(1 + O(e^4, \lambda^2)\right),\tag{53}$$

in agreement with a recent calculation of Arnold [23]. Note, that there is no correction of order $\lambda^{3/2}$. In addition, for temperatures above T_b' the limit $\phi \to 0$ can now be taken in the equation for the transverse photon mass, yielding $m_T^2 = 0$. The difference with respect to the case discussed in sect. 2 (cf. eq. (20)) is due to the summation of "daisy" graphs for the photon plasma mass which correspond to "superdaisy" contributions to the potential. These graphs yield a nonvanishing, real plasma mass m_ϕ which now appears on the RHS of eq. (43).

Away from the origin, at $\phi > 0$, terms proportional to T/m_i become important in the gap equations. These terms reflect the expected infrared divergencies in finite-temperature perturbation theory which appear if zero mass excitations are present. Inspection of eqs. (42)–(45) suggests that perturbation theory is reliable if the following inequalities are satisfied:

$$\xi\frac{2e^2}{3\pi}\frac{T}{m_T + m_\phi} \leqslant 1, \tag{54}$$

$$\xi\frac{\lambda T}{12\pi}\left(\frac{9}{m_\phi} + \frac{1}{m_\chi}\right) \leqslant 1. \tag{55}$$

The first inequality stems from the equation for m_T^2 and the second from the equation for m_ϕ^2. We do not know how well the perturbation series converges without a complete calculation to $O(e^4, \lambda^2)$. Hence, we have included a factor ξ which ensures that leading terms of order e^2 and λ are ξ times larger than next-to-leading terms of order e^3 and $\lambda^{3/2}$, respectively. The dependence of our results on ξ indicates the influence of unknown higher-order corrections.

Close to the origin, at $\phi \approx 0$, the above conditions imply that one cannot even reach the barrier temperature T_b'. Eqs. (48), (54) and (55) yield the lower bounds on the temperature T, $T > T_V$ and $T > T_S$, where

$$\frac{T_V^2 - T_b^2}{T_V^2} = \frac{16\xi^2 e^4}{3\pi^2(3e^2 + 4\lambda)}, \tag{56}$$

and

$$\frac{T_S^2 - T_b^2}{T_S^2} = \frac{25\xi^2\lambda^2}{3\pi^2(3e^2 + 4\lambda)}. \tag{57}$$

Here, the subscript "V" ("S") indicates that the infrared divergence fo the vector (scalar) field plasma mass sets the temperature. Our expression for the effective potential is therefore only reliable for temperatures above T^*, which denotes the largest temperature among T_b', T_V and T_S.

Let us now turn to the validity of $V(\phi, T)$ at $\phi \neq 0$. Eqs. (42) and (43) show that the plasma masses m_L and m_T are well-behaved for all values of ϕ. However, m_ϕ^2 and m_χ^2 vanish at the turning points and at the extrema of the potential according to eqs. (49) and (50) and become negative beyond these points. To the order in which we are working this is not visible in the potential because only the lowest-order plasma masses, given in eqs. (48), enter. Nevertheless, eq. (55) indicates the appearance of infrared divergences in the next order. Hence, we can rely on the potential only a little away from turning points and extrema such that the condition (55) is met.
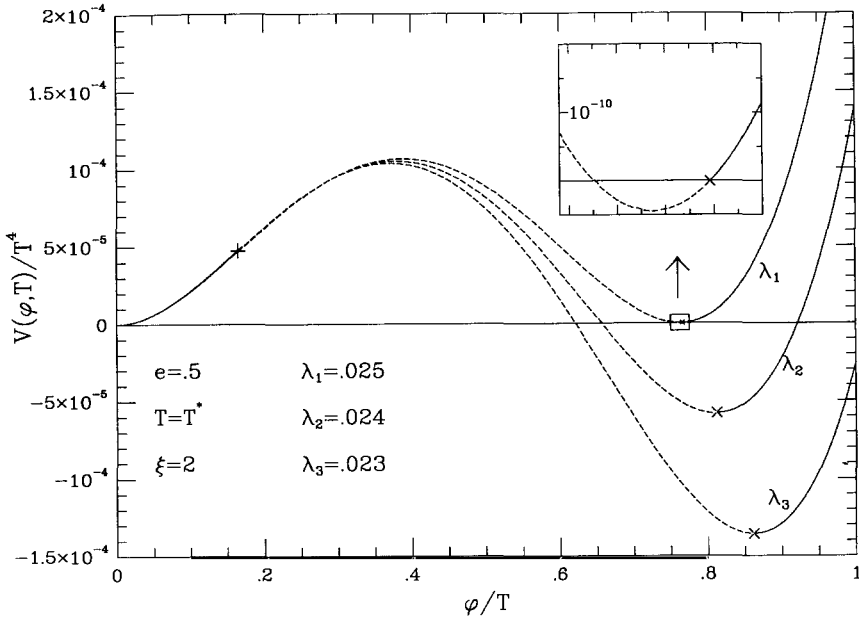
Fig. 8. The effective potential to order e^3 and $\lambda^{3/2}$ for different values of λ at the smallest temperatures T^* which are compatible with perturbation theory. The parts with broken lines are not reliable due to imaginary masses.

These restrictions are illustrated in fig. 8 where we have plotted $V(\phi, T)$ at the smallest allowed temperature T^* for some values of λ. Whenever perturbation theory is trustworthy a solid line is drawn and a broken line otherwise. At the upright cross " + " and the tilted cross " × " m_ϕ and m_χ, respectively, have reached their smallest values compatible with eq. (55). We denote the value of the scalar field at the tilted cross $\phi_\times$.

In order to establish the existence of a first-order phase transition we have to show that a critical temperature $T_c' > T^*$ exists, such that at temperatures T between T_c' and T^* the effective potential has a global minimum at an expectation value $\phi(T) > 0$. In particular, one has

$$V(\phi^*, T^*) \leqslant V(0, T^*), \quad \phi^* = \phi(T^*). \tag{58}$$

Here V, ϕ^* and T^* depend upon the couplings, and in this way we can find a region in the plane of couplings e^2 and λ where the symmetric phase is metastable. As illustrated in fig. 8, as λ increases, $V(\phi^*, T^*)$ increases as well and eventually becomes degenerate with $V(0, T^*)$ at $\lambda =: \bar{\lambda}$. Repeating this procedure numerically for different values of e^2 yields a boundary $\bar{\lambda}(e^2)$ for the region of metastability.
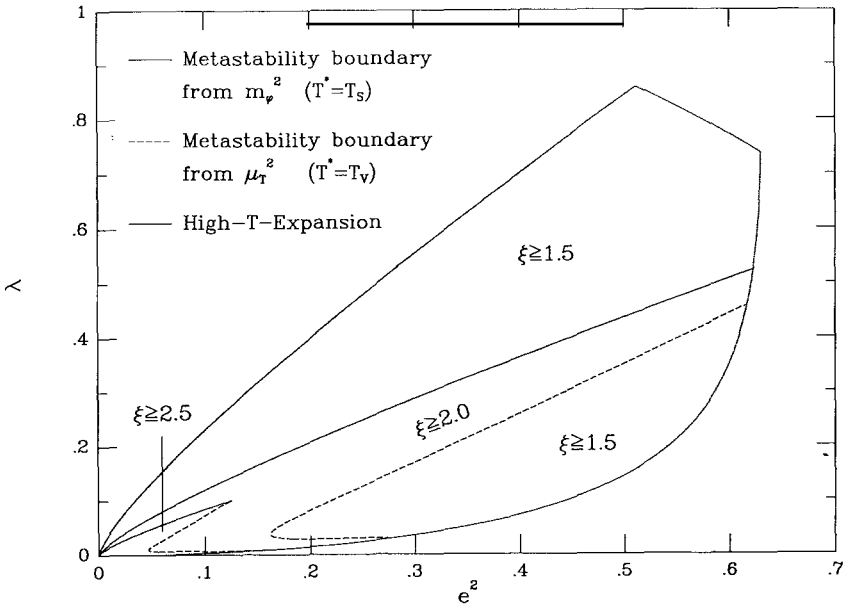
Fig. 9. Regions in coupling space where we can establish metastability of the symmetric phase. They depend on the convergence parameter ξ.

So far we have ignored the breakdown of perturbation theory at large values of ϕ. Because of condition (55) λ must not be increased until the two minima of V become degenerate but only until

$$V(0, T^*) = V(\phi_\times, T^*).$$ (59)

The numerical difference is tiny (cf. the blown up box in fig. 8), and the boundary $\bar{\lambda}(e^2)$ remains essentially unchanged.

The resulting regions of metastability are shown in fig. 9. The solid curves are the boundaries at $T^* = T_S$ for different values of the convergence factor ξ. The dotted curves indicate the convergence of the high-temperature expansion for which we require

$$\frac{m_i(\phi_\times, T_c')}{T_c'} < 0.5.$$ (60)

The corresponding error in the effective potential is less than 1%. The region bounded by these two curves contains pairs of couplings (e^2, λ) which guarantee metastability of the symmetric phase as long as $\xi < 1.8$. Once ξ becomes larger and the requirements on the convergence of the perturbation series more stringent, the broken curve with $T^* = T_V$ crosses the dotted high-temperature line and

excludes the region to its right. The quite unexpected shape of the broken curve which intersects lines $e^2 = $ const. twice traces back to the dependence of T'_c and T_V upon λ for fixed e^2. It turns out that T'_c has a minimum whereas eq. (56) shows that T_V decreases monotoneously, and at sufficiently large ξ the temperatures T'_c and T_V intersect twice. In scalar electrodynamics with N scalar fields regions of metastability have recently been determined by Jain [24] using different techniques.

As an example, for a convergence factor $\xi = 2$, the largest permissible ratio of scalar mass to vector boson mass is

$$\frac{m_S}{m_V} = \frac{\overline{m}_\phi(\phi = 0)}{ev} = \frac{\sqrt{2\lambda}}{e} \approx 1.3. \tag{61}$$

The region of metastability shrinks drastically as ξ increases, and we cannot even reach the vector boson mass $m_V = ev = 90$ GeV. Note, that this rather stringent bound arises from infrared divergencies affecting m_T^2.

The main result of this section, the regions of metastability shown in fig. 9, strongly depends on the value of ξ, i.e., on our assumption on the convergence of the perturbation series. Our results may be improved in several ways. First, the proper values of ξ are presumably different for eq. (54) and eq. (55) because the effect of m_T^2 on the potential is of higher order in the couplings. Furthermore, the most stringent constraints are derived at $\phi \approx 0$ where one may hope to improve the convergence by means of the renormalization group and by evaluating the gap equations at finite momentum. We plan to discuss these problems in more detail elsewhere.

5. Decay of metastable states

In condensed matter physics the decay of metastable states is described by Langer's theory [17,18]. Here the starting point is a coarse-grained free energy $F_\Lambda[c, T]$ of the type shown in fig. 10, where a local metastable minimum and the
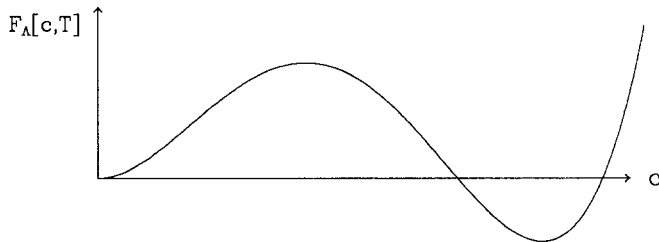

Fig. 10. Typical coarse-grained free energy $F_\Lambda[c, T]$ as functional of the order parameter c.

global minimum are separated by a barrier; c is the order parameter of the system under consideration and Λ is the coarse-graining scale. Based on an investigation of the Fokker–Planck equation for the probability distribution of large fluctuations of the order parameter ("subcritical droplets") Langer obtained the following relation for the decay rate [18]:

$$\Gamma = \frac{\kappa}{2\pi} \frac{\mathrm{Im}\, Z_\beta[\bar{c}]}{Z_\beta[c=0]}, \tag{62}$$

with

$$Z_\beta[c] = \mathrm{e}^{-\beta F[c,T]}, \tag{63}$$

where $F[c, T]$ is the total free energy of the configuration c, and κ is a dynamic factor which cannot be obtained from equilibrium thermodynamics; $c = 0$ corresponds to the homogeneous metastable state and $\bar{c}(x)$ is a configuration which interpolates between $c = 0$ at $|x| \to \infty$ and the global minimum at $x = 0$. The imaginary part in eq. (62) reads explicitly

$$\mathrm{Im}\, Z_\mathrm{b}[\bar{c}] = \frac{1}{\sqrt{|\bar{\lambda}_-|}} \mathscr{V} \prod_i {}^{>} \left(\bar{\lambda}_i \right)^{-1/2} \mathrm{e}^{-\beta F_\Lambda[\bar{c},T]}, \tag{64}$$

where $\bar{c}$ is a stationary point of F_Λ,

$$\left. \frac{\delta F_\Lambda[c, T]}{\delta c(x)} \right|_{c=\bar{c}} = 0, \tag{65}$$

$\Pi^{>}$ denotes the product of all positive eigenvalues $\bar{\lambda}_i$ of fluctuations around $\bar{c}$, $\bar{\lambda}_-$ is the single negative eigenvalue, and $\mathscr{V}$ is the volume of zero-modes associated with the symmetries of the system under consideration.

How can we apply this formalism to the decay of the metastable symmetric phase in scalar electrodynamics? In analogy to eq. (62) the decay rate is given by

$$\Gamma = \frac{\kappa}{2\pi} \frac{\mathrm{Im}\, Z_\beta[\bar{\Phi}]}{Z_\beta[\Phi=0]}, \tag{66}$$

with

$$Z_\beta[\Phi] = \mathrm{e}^{-\beta F[\Phi,T]}$$

$$= \int_\beta [\mathrm{D}\hat{\Phi}][\mathrm{D}A_\mu] \delta(f) \det \frac{\partial f}{\partial \alpha}$$

$$\times \exp\left[-\left(S_\beta[\Phi + \hat{\Phi}, A_\mu] - \int_\beta \mathrm{d}x \frac{\delta F[\Phi, T]}{\delta \Phi(x)} \hat{\Phi}(x) \right) \right]. \tag{67}$$

Here $\overline{\Phi}$ is again a field configuration which interpolates between the symmetric and the broken phase. $\Phi = 0$ and $\overline{\Phi}$ are approximate stationary points of the free energy $F[\Phi, T]$. Hence, we neglect the second term of the integrand in eq. (67).

The functional integrals over the vector field yields an effective action which depends on the scalar field $\Phi + \hat{\Phi}$,

$$\int_{\beta} [\mathrm{D}A_{\mu}] \delta(f) \det \frac{\partial f}{\partial \alpha} e^{-S_{\beta}[\Phi + \hat{\Phi}, A_{\mu}]}$$

$$= \exp\left(- \int_{\beta} \mathrm{d}x \left(\partial_{\mu}(\Phi + \hat{\Phi}) \partial^{\mu}(\Phi + \hat{\Phi}) \right. \right.$$

$$\left. \left. - V_0(z) - V_1(z, T) + Z_1(z, T) \partial_{\mu}(\Phi + \hat{\Phi}) \partial^{\mu}(\Phi + \hat{\Phi}) + \ldots \right) \right), \quad (68)$$

where $z = \sqrt{2} |\Phi + \hat{\Phi}|$. $V_1(z, T)$ is the familiar contribution of vector loops to the one-loop effective potential (cf. eq. (5)). In the following we will neglect the wave function correction $Z_1(z, T)$.

The integral over the scalar field fluctuations $\hat{\Phi}$ can now be carried out in the saddle point approximation. As discussed in sect. 2, $\phi = 0$ and $\phi_+(T)$ are the two local minima of the potential $V_A = V_0 + V_1$. In the thin wall approximation [25] the stationary point of the "vector loop" free energy

$$F_A[\Phi, T] = \int \mathrm{d}^3x \left(|\nabla \Phi|^2 + V_A(z, T) \right) \quad (69)$$

is given by

$$\overline{\Phi}(r) = \frac{1}{\sqrt{2}} \overline{\phi}(r) = \frac{1}{2\sqrt{2}} \phi_+(T) \left[1 - \tanh\left(\frac{r - R(T)}{d(T)} \right) \right], \quad (70)$$

with

$$d(T) = \frac{2\sqrt{2}}{\sqrt{\lambda} \, \phi_+(T)},$$

$$\sigma(T) = \int_0^{\phi_+(T)} \mathrm{d}\phi \sqrt{2V_A(\phi, T)},$$

$$R(T) = \frac{2\sigma}{\epsilon(T)}, \quad \epsilon = V_A(0, T) - V_A(\phi_+(T), T). \quad (71)$$

The free energy $F_A[\overline{\Phi}, T]$ is then the sum of a volume term and a surface term:

$$F_A[\overline{\Phi}, T] = 4\pi R^2(T)\sigma - \tfrac{4}{3}\pi R^3(T)\epsilon(T). \tag{72}$$

It is sufficient to evaluate the surface tension σ at the critical temperature T_c.

The scalar fluctuations $\hat{\Phi}$ consist of the radial modes $\hat{\phi}$ and the Goldstone modes $\hat{\chi}$ ($\overline{\phi} = \sqrt{2}\ \overline{\Phi}$):

$$F_A[\overline{\Phi} + \hat{\Phi}, T] = F_A[\overline{\Phi}, T] + \tfrac{1}{2}\int_\beta dx\ dy\ \hat{\phi}(x)\frac{\delta^2 F_A[\overline{\Phi}, T]}{\delta\phi(x)\ \delta\phi(y)}\hat{\phi}(y)$$

$$+ \tfrac{1}{2}\int_\beta dx\ dy\ \hat{\chi}(x)\frac{\delta^2 F_A[\overline{\Phi}, T]}{\delta\chi(x)\ \delta\chi(y)}\hat{\chi}(y). \tag{73}$$

The corresponding potentials for the scalar fields $\hat{\phi}$ and $\hat{\chi}$ are

$$U_\phi(r) = \left.\frac{\partial^2}{\partial\phi^2}V(\phi, T)\right|_{\phi = \overline{\phi}(r)}, \tag{74}$$

$$U_\chi(r) = \left.\frac{1}{\phi}\frac{\partial}{\partial\phi}V(\phi, T)\right|_{\phi = \overline{\phi}(r)}. \tag{75}$$

Both potentials are plotted in fig. 11. The spectrum of eigenvalues contains four zero-modes, three translational invariance and one for the global U(1)-symmetry of $F_A[\Phi, T]$.

The discrete $\hat{\phi}$ spectrum is well known [17,26], since the bound states are localized at $r \approx R$. There is one negative eigenvalue,

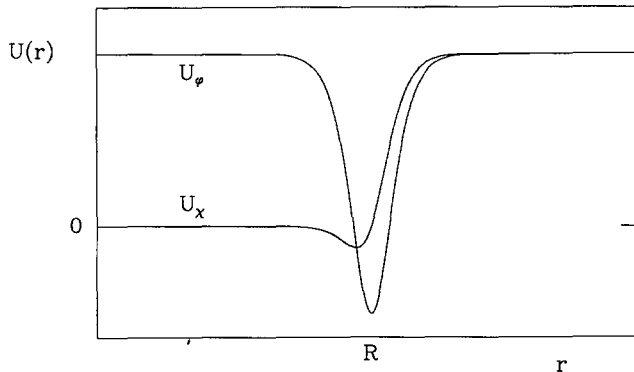$$\lambda_- = \lambda_{000} \approx -\frac{2}{R^2}, \tag{76}$$

Fig. 11. The potentials $U_\phi(r)$ and $U_\chi(r)$ for the scalar fluctuations $\hat{\phi}$ and $\hat{\chi}$.

which guarantees that $Z_\beta[\overline{\Phi}]$ is purely imaginary. Furthermore, there are "Goldstone modes" λ_{0lm} which correspond to deformations of the droplet surface [17,26,27],

$$\lambda_{0lm} \approx \frac{(l-1)(l+2)}{R^2}. \tag{77}$$

Here l and m label the three-dimensional spherical harmonics. The three zero eigenvalues λ_{01m} are the zero-modes of translational invariance. $\hat{\chi}_0 \sim \overline{\phi}$ is the zero-mode of the U(1)-symmetry. A straightforward calculation yields for the corresponding phase space volumes:

$$\mathscr{V}_\phi = \left(\frac{\beta}{2\pi} F_A[\overline{\Phi}, T]\right)^{3/2} V,$$

$$\mathscr{V}_\chi = 2\pi \left(\frac{\beta}{2\pi} \int \mathrm{d}^3x \, \overline{\phi}^2\right)^{1/2}, \tag{78}$$

where V is the total volume of the physical three-dimensional space. For the product of the low-lying "Goldstone modes" one can obtain a closed expression [17,27,28]:

$$\prod_{\lambda_{0lm} < \mu^2} \left(\frac{1}{\mu^2}\lambda_{0lm}\right)^{1/2} \approx (\mu R)^{-5/3}, \tag{79}$$

where $\mu = m_\phi(0, T)$. Combining eqs. (66), (72) and (76)–(79) we finally arrive at the transition rate

$$\frac{\Gamma}{V} = \frac{\sqrt{2}}{9\pi} \frac{e^3}{\lambda} \kappa (\beta\sigma)^{3/2} (\beta\mu)^{-1/2} (R\mu)^{23/6} \exp\left(-\tfrac{4}{3}\pi\beta\sigma R^2\right). \tag{80}$$

Here the contributions of zero-modes and Goldstone modes to the determinant of scalar fluctuations around the saddle point have been taken into account. The "dynamical factor" κ has recently been related to plasma viscosities [29].

Eq. (80) gives the decay rate of the metastable symmetric phase according to Langer's theory of metastability. The free energy $F_A[\Phi, T]$, obtained by integrating out the vector field A_μ, plays the role of the coarse-grained free energy $F_A[c, T]$ in condensed matter physics. An important aspect of this approach is that scalar fluctuations are only computed around the stationary points $\Phi = 0$ and $\Phi = \overline{\Phi}$ of $F_A[\Phi, T]$ and *not*, as usually done, around unstable homogeneous scalar background fields. Hence, perturbation theory is consistent and does not break down due to infrared divergencies or negative scalar mass terms. The decay rate (80) is

similar to the results previously obtained by Linde [25]. There are, however, some qualitative differences with respect to the treatment of scalar fluctuations, the negative eigenvalue and the occurrence of a dynamical pre-factor κ.

In our approach an approximate free energy, which yields the non-trivial saddle point, is obtained by first integrating out the vector field. Alternatively one could try to first integrate out high-momentum modes with $k^2 > \Lambda^2$ for scalar and vector fields (cf. refs. [30,31]). The corresponding free energy F_Λ, where Λ is now an infrared cutoff, should exhibit a barrier between a stable and a metastable extremum. Low-momentum modes with $k^2 < \Lambda^2$ should then yield the interpolating configuration $\bar{\phi}$. Such a cutoff Λ must not destroy the effect of the cubic term in the effective potential, which implies $\Lambda^2 < \zeta e^2 \phi_+^2$, $\zeta \ll 1$. Furthermore, $\bar{\phi}$ must be essentially homogeneous for distances $r < 1/\Lambda$, i.e., $\Lambda^2 > 1/d^2 \sim \lambda \phi_+^2$ (cf. eq. (71)). Both conditions together require $\lambda/e^2 < \zeta$, which can indeed be satisfied for the range of λ and e^2 identified in sect. 4. Since $\phi_+ \approx e^3 T/(2\pi\lambda)$, one may choose $\Lambda^2 < e^2 T^2$. In this case we expect plasma masses to appear in the free energy F_Λ. Correspondingly, one should include in the evaluation of the decay rate eq. (80) plasma mass effects, which essentially reduce the cubic term in the effective potential by $\frac{1}{3}$ [7].

Let us finally examine whether our approach can consistently describe a first-order cosmological phase transition. A rough estimate of the temperature T_e at which the phase transition ends, is obtained by requiring

$$\Gamma(t_e) t_e^4 \sim 1, \tag{81}$$

where $t \approx 0.03 m_{pl}/T^2$ (cf. ref. [32]). In table 1 we compare three examples of couplings for which perturbation theory is consistent if $\xi \leqslant 1.8$. They are evaluated at $e^2 = 0.32$, where $m_V = 90$ GeV for a choice of $v = 160$ GeV. The self-coupling λ is chosen such that the scalar masses $m_S = \sqrt{2}\,\lambda v$ are $m_S = 60$ Gev, $m_S = m_V = 90$ GeV and $m_S = 120$ GeV. The latter is close to the largest scalar self-coupling which satisfied the bounds in fig. 9 for $\xi = 2$. All temperatures, the surface tension σ, the droplet radius R, the correlation length $1/\mu$ and the droplet thickness d have been extracted from the "vector loop" potential V_Λ in eq. (69). In parentheses we added their relative deviation from values that stem from the full potential

TABLE 1
Observables of first-order phase transitions for $e^2 = 0.32$ and three different values of λ (see text).

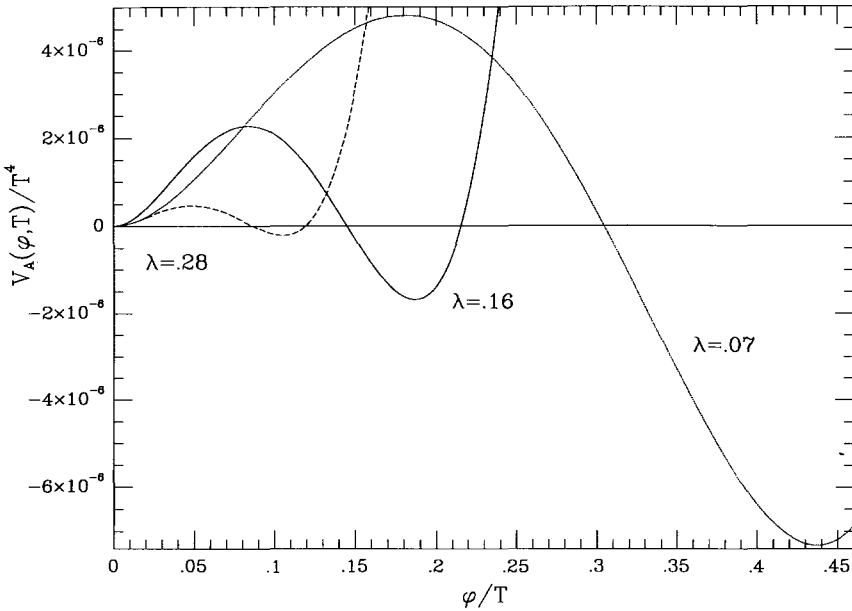| λ	T_c (GeV)	$T_c - T_e$ (GeV)	$T_c - T_b$ (GeV)	σ (10^3 GeV)^3	R^{-1} (GeV)	$1/R\mu$	d/R
0.07	150 (8%)	0.41 (37%)	6 (37%)	8 (40%)	1.3	0.11	0.28
0.16	230 (18%)	0.14 (29%)	4 (40%)	3 (25%)	0.67	0.06	0.15
0.28	300 (27%)	0.07 (14%)	3 (29%)	2 (36%)	0.44	0.04	0.10

Fig. 12. The "vector loop" potential for the values of λ given in table 1 at the corresponding temperature $T_{\rm e}$. The potential with $\lambda = 0.07$ has been reduced by a factor of five.

V in eq. (51). They illustrate the uncertainty due to unknown higher-order corrections.

Table 1 shows to what extend the thin wall approximation is valid. The ratios d/R appear acceptable for $\lambda = 0.16$ and $\lambda = 0.28$ whereas the case $\lambda = 0.07$ is marginal. Note, that this value of λ is not contained in the metastability region for $\xi = 2$. In all cases the critical radius is much larger than the correlation length $1/\mu$. We have compared the exact saddle point free energy (cf. ref. [7,25]) with its thin wall approximation. For all values of λ the difference is less than 7%. Also the semiclassical approximation appears to be accurate. For $\Gamma/(VT^4)$ the correction of the calculation pre-factor to the saddle point free energy is about 1%. In fig. 12 the "vector loop" free energy is shown as function of ϕ for the three values of λ at the corresponding temperatures $T_{\rm e}$ where the phase transition is completed (cf. table 1). For $\lambda = 0.16$ and $\lambda = 0.28$ the barrier height is larger than the depth of the global minimum. This further supports the validity of the thin wall approximation for these values of λ.

To conclude, we have obtained a consistent description of a cosmological first-order phase transition for values of e^2 and λ within the $\xi = 2$ metastability region. However, the transition is only weakly first order, and its cosmological implications remain uncertain at present.

6. Summary

In the previous sections we have studied the transition from the symmetric to the broken phase in scalar electrodynamics at finite temperature. We have seen that, due to infrared divergencies, ordinary perturbation theory to finite order in e and λ does not yield a useful approximation to the effective potential. However, an improved perturbation theory, which takes plasma masses into account, describes consistently the symmetric phase ($\phi = 0$) and also the broken phase ($\phi > 0$) in the neighbourhood of the second non-trivial, local minimum of the effective potential. Using this improved perturbation theory we have evaluated the effective potential including all terms of order e^3 and $\lambda^{3/2}$. To this order all contributions linear in ϕ cancel.

The plasma masses have been determined from a set of one-loop gap equations which also yield the range in the couplings e and λ, the temperature T and the scalar field ϕ where the perturbation series converges. Knowing the range in T and ϕ as function of e and λ where the effective potential is reliable has allowed us to determine the range in e and λ where the symmetric phase is metastable. As a criterion we required the effective potential at the origin, $\phi = 0$, to have only a local and not a global minimum for the allowed values of T. In sect. 3 an important technical point has been the derivation of the correct relations between longitudinal and transverse plasma masses and the photon self-energy in the case of spontaneous symmetry breaking.

Following the theory of Langer we have finally computed the nucleation rate for critical droplets. We have argued that the effective action, obtained by integrating out the vector field, plays the role of the coarse-grained free energy in condensed matter physics. Here a necessary condition is $\lambda \lesssim e^2$ which is satisfied within the regions of metastability found in sect. 4. Scalar fluctuations are only computed around the critical droplet and not around unstable homogeneous scalar background field. Hence, the usual problems related to infrared divergencies and imaginary scalar masses are absent. We have also shown that for Higgs boson masses of the order of the vector boson mass a cosmological phase transition would indeed by first order, i.e., it would proceed via nucleation and growth of critical droplets. Since the transition is only weakly first order, its cosmological implications remain rather uncertain at present.

Our results could be improved in several respects. First, it is important to replace our criterion for the convergence of the perturbation series, which we obtained by inspection of the gap equations, by a complete computation of the effective potential to order e^4, λ^2. This is necessary in order to be sure about the range of parameters for which perturbation theory is reliable. Furthermore, the validity of the expansion in powers of derivatives used in sect. 5 and the validity of the thin wall approximation have to be examined in greater detail. Finally, it would be interesting to study a renormalization group improved version of the gap equations and eventually the full Schwinger–Dyson equations.

An extension of our approach to the electroweak phase transition is in principle straightforward. We will report on our results in a forthcoming publication.

References

[1] D.A. Kirzhnits and A.D. Linde, Phys. Lett. B72 (1972) 471
[2] S. Weinberg, Phys. Rev. D9 (1974) 3357
[3] L. Dolan and R. Jackiw, Phys. Rev. D9 (1974) 3320
[4] D.A. Kirzhnits and A.D. Linde, JETP Lett. 40 (1974) 628
[5] V.A. Kuzmin, V.A. Rubakov and M.E. Shaposhnikov, Phys. Lett. B155 (1985) 36
[6] K. Enqvist et al., Phys. Rev. D45 (1992) 3415
[7] M. Dine et al., Phys. Rev. D46 (1992) 550
[8] M.E. Carrington, Phys. Rev. D45 (1992) 2933
[9] C.G. Boyd, D.E. Brahm and S.D.H. Hsu, Caltech preprint CALT-68-1795 (1992)
[10] M.E. Shaposhnikov, Phys. Lett. B277 (1992) 324 [Erratum B282 (1992) 483]
[11] M. Gleiser, E.W. Kolb and R. Watkins, Nucl. Phys. B364 (1991) 411
[12] N. Tetradis, Z. Phys. C57 (1993) 331
[13] M. Gleiser and E.W. Kolb, Phys. Rev. Lett. 69 (1992) 1304
[14] M. Gleiser and E.W. Kolb, preprint FERMILAB-Pub-92/222-A
[15] D.A. Kirzhnits and A.D. Linde, Ann. Phys. 101 (1976) 195
[16] A.D. Linde, Rep. Prog. Phys. 42 (1979) 389
[17] J. Langer, Ann. Phys. 41 (1967) 108
[18] J. Langer, Ann. Phys. 54 (1969) 258
[19] J.I. Kapusta, Finite temperature field theory (Cambridge U.P., 1989)
[20] R. Jackiw, Phys. Rev. D9 (1974) 1686.
[21] S. Weinberg, Phys. Rev. Lett. 36 (1976) 294;
     A. Linde, Phys. Lett. B70 (1977) 306
[22] K. Takahashi, Z. Phys. C26 (1985) 601
[23] P. Arnold, Phys. Rev. D46 (1992) 2628
[24] V. Jain, Max Planck Institute preprint MPI-Ph/92-72 (1992)
[25] A.D. Linde, Nucl. Phys. B216 (1983) 421
[26] C. Callan and S. Coleman, Phys. Rev. D16 (1977) 1762
[27] N.J. Günther, D.A. Nicole and D.J. Wallace, J. Phys. A (Math. Gen.) 13 (1980) 1755
[28] W. Buchmüller and T. Helbig, in preparation
[29] L.P. Csernai and J.I. Kapusta, Phys. Rev. D46 (1992) 1379
[30] C. Wetterich, Nucl. Phys. B352 (1991) 529;
     N. Tetradis and C. Wetterich, Nucl. Phys. B398 (1993) 659
     G. Mack et al., DESY preprint DESY 92-070 (1992)
[31] L.D. Landau and E.M. Lifshitz, Statistical physics, part 1, 3rd edition (Pergamon, Oxford, 1980) ch. 147;
     J.S. Langer, Physica 73 (1974) 61
[32] W. Buchmüller and T. Helbig, Int. J. Mod. Phys. C3 (1993) 799